Cell Reports

Supplemental Information

cKit Lineage Hemogenic Endothelium-Derived Cells Contribute to Mesenteric Lymphatic Vessels

Lukas Stanczuk, Ines Martinez-Corral, Maria Ulvmar, Yang Zhang, Bàrbara Laviña, Marcus Fruttiger, Ralf H. Adams, Dieter Saur, Christer Betsholtz, Sagrario Ortega, Kari Alitalo, Mariona Graupera, and Taija Mäkinen

A

Stage	Genotype				
	Wt	*p110α*$^{D933A/+}$	*Vegfr3*$^{lz/+}$	*Vegfr3*$^{lz/+}$; *p110α*$^{D933A/+}$	Total
E13-E18	21 (21%)	31 (32%)	22 (22%)	25 (26%)	98
P0-P7	29 (34%)	31 (36%)	15 (17%)	11 (13%)	86
P21	4 (45%)	2 (22%)	3 (33%)	0 (0%)	9
Expected	25%	25%	25%	25%	

B

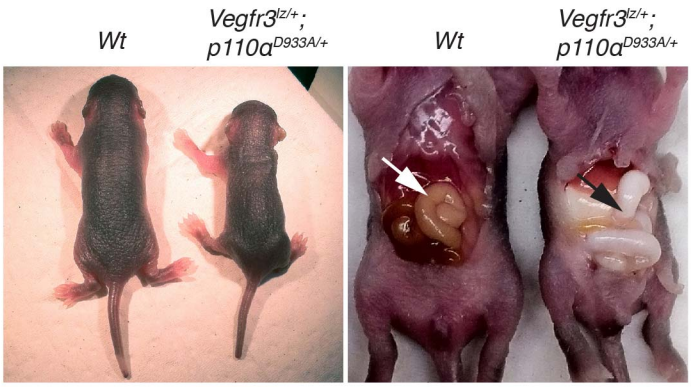

C

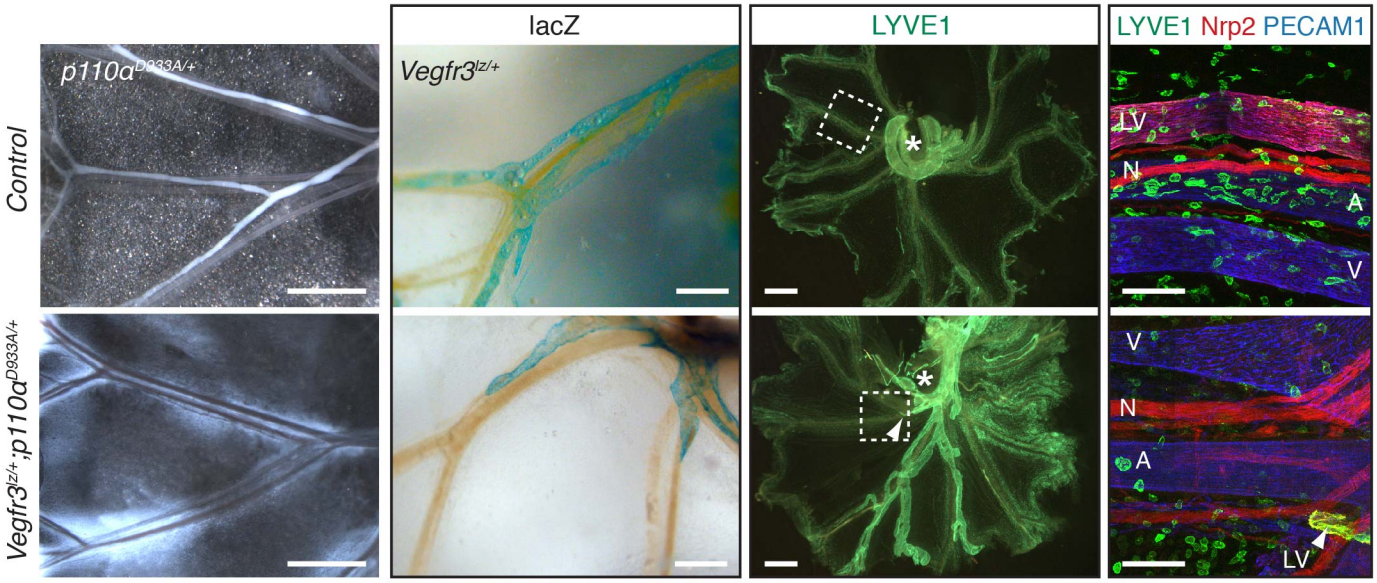

D

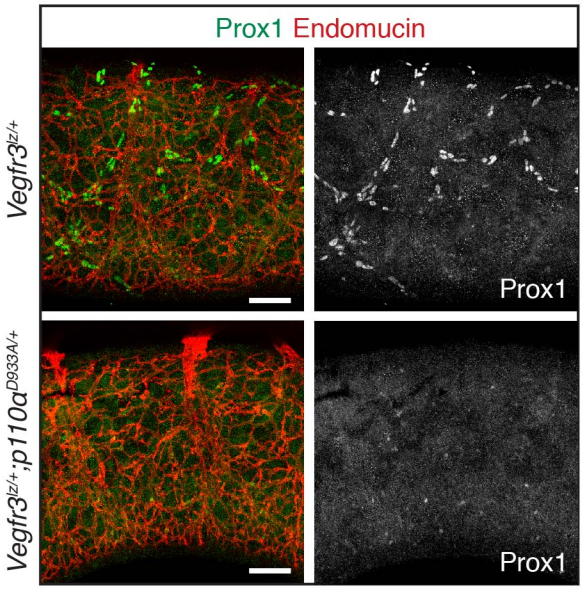

E

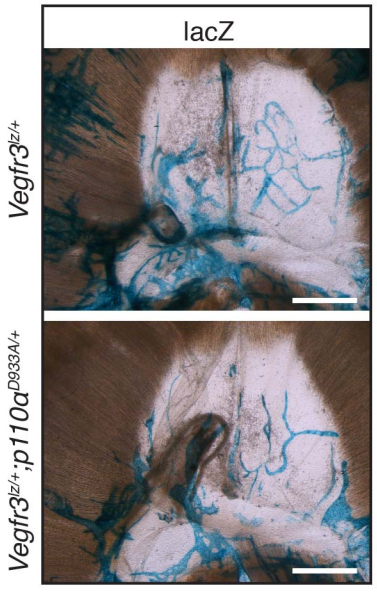

Figure S1

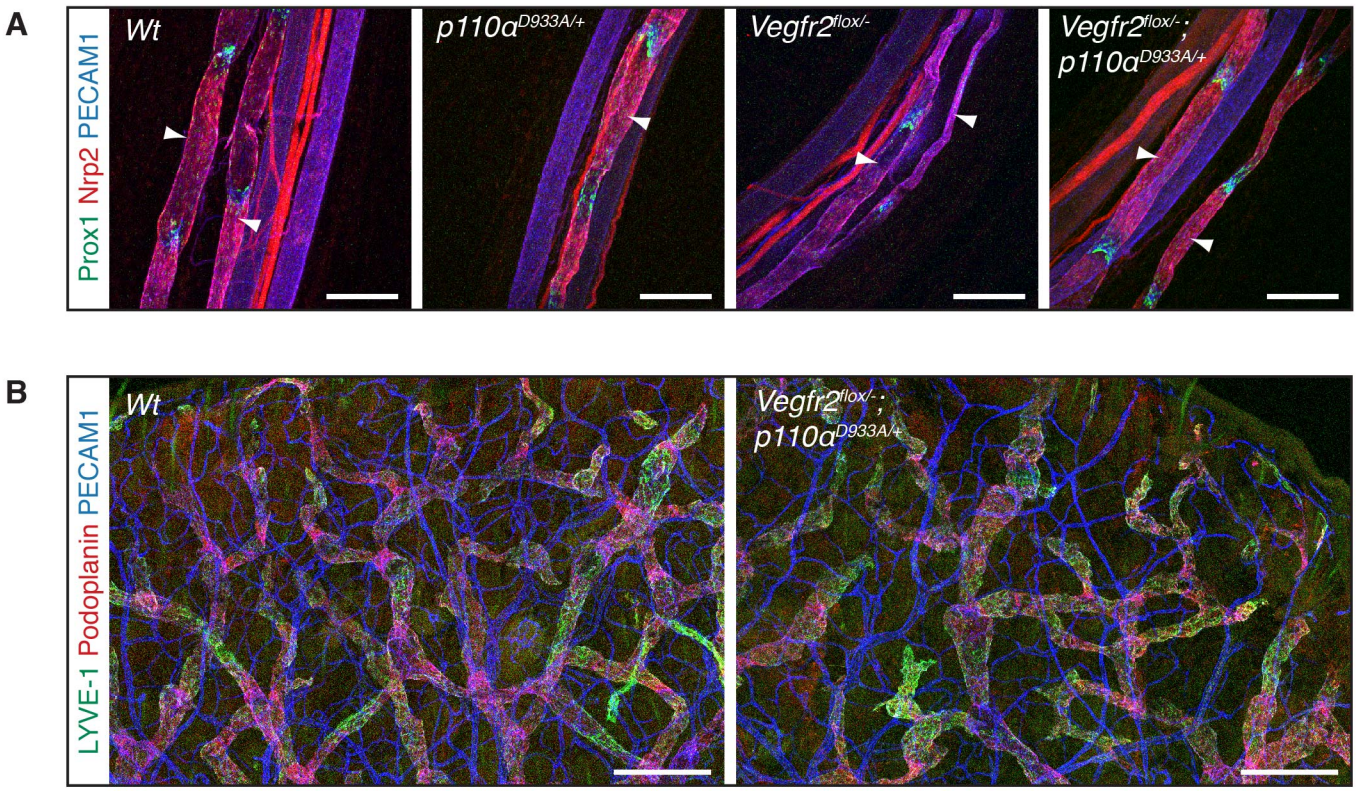
A
Prox1 Nrp2 PECAM1
Wt
p110α D933A/+
Vegfr2 flox/-
Vegfr2 flox/-; p110α D933A/+
B
LYVE-1 Podoplanin PECAM1
Wt
Vegfr2 flox/-; p110α D933A/+

Figure S2

A

FACS analysis of skin EC from E15.5 *Vegfr3-CreER^{T2};R26-mTmG*

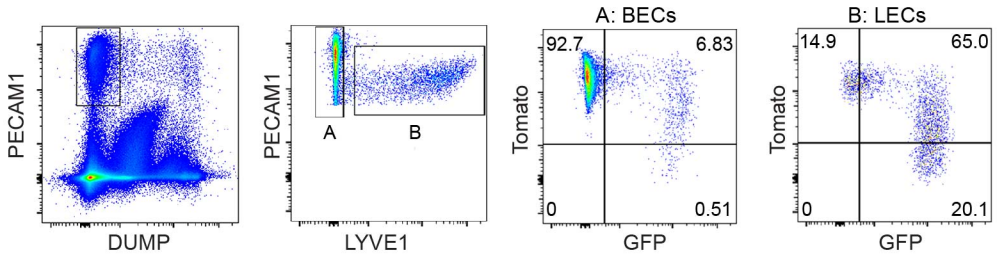

B

FACS analysis of mesenteries and intestinal ECs from E17.5 *Vegfr3-CreER^{T2};R26-mTmG*

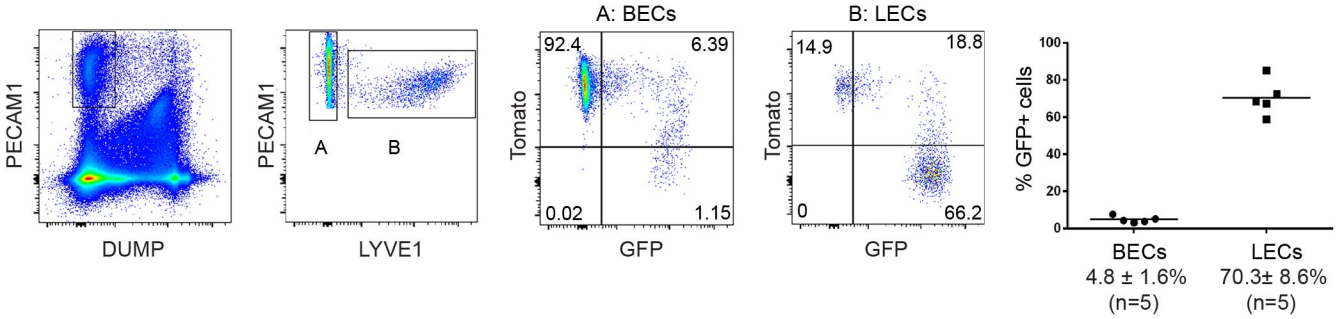

FACS analysis of skin EC from E17.5 *Vegfr3-CreER^{T2};R26-mTmG*

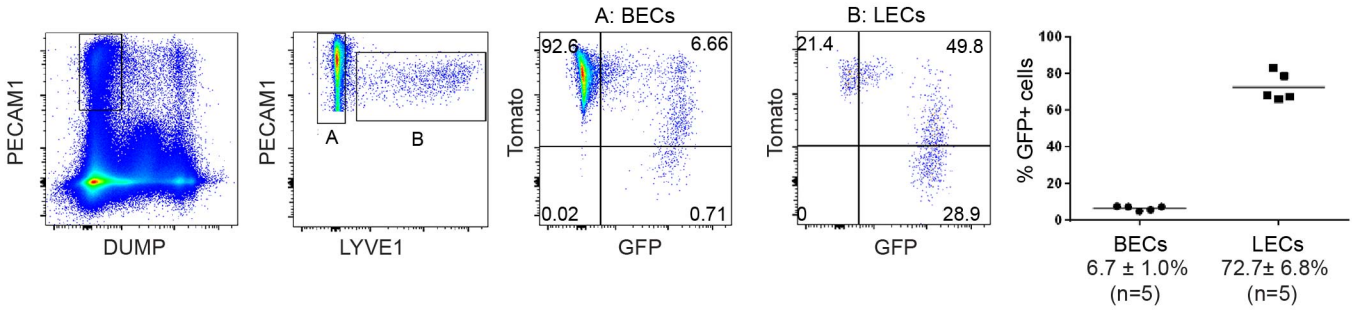

Figure S3

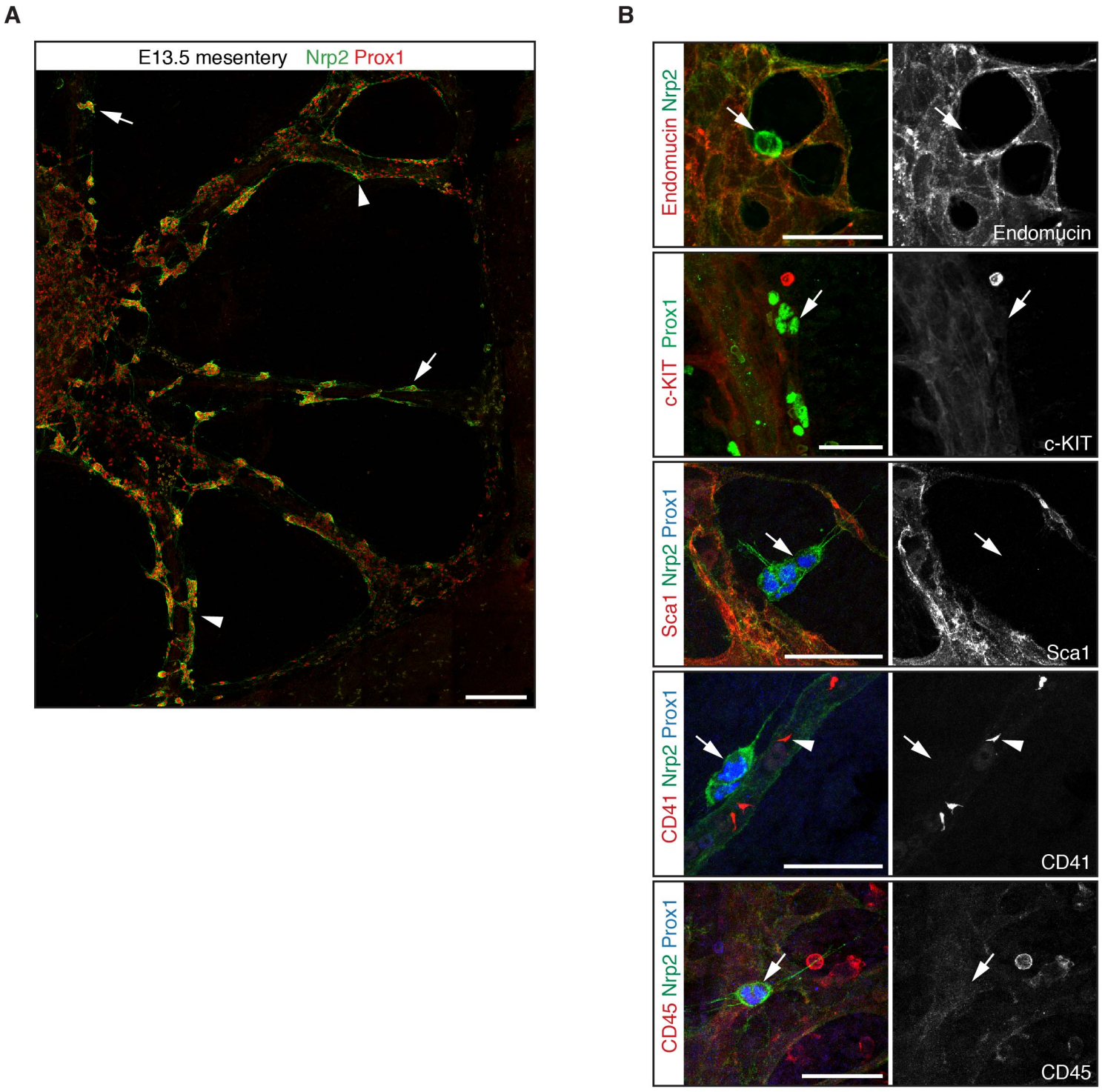
A
E13.5 mesentery Nrp2 Prox1
B
Endomucin Nrp2
Endomucin
c-KIT Prox1
c-KIT
Sca1 Nrp2 Prox1
Sca1
CD41 Nrp2 Prox1
CD41
CD45 Nrp2 Prox1
CD45

Figure S4

A

induction	GFP labeling in mesentery				number of		% embryos with LEC labeling
	artery	vein	lymphatic	HC	embryos	litters	
E8	(+)	-	- / + / ++	+++	4	2	50
E9	+++	+	- / +	++	3	2	67
E8+E9	+++	++	+ / ++	+++	3	3	100
E10	+++	+	+	(+)	2	2	100
E10+E11	+++	++	+	(+)	2	2	100
E11+E12	+++	++	(+)	- / (+)	3	3	100
E13	+++	++	(+)	-	2	1	100
E14	+++	++	(+)	-	2	1	100

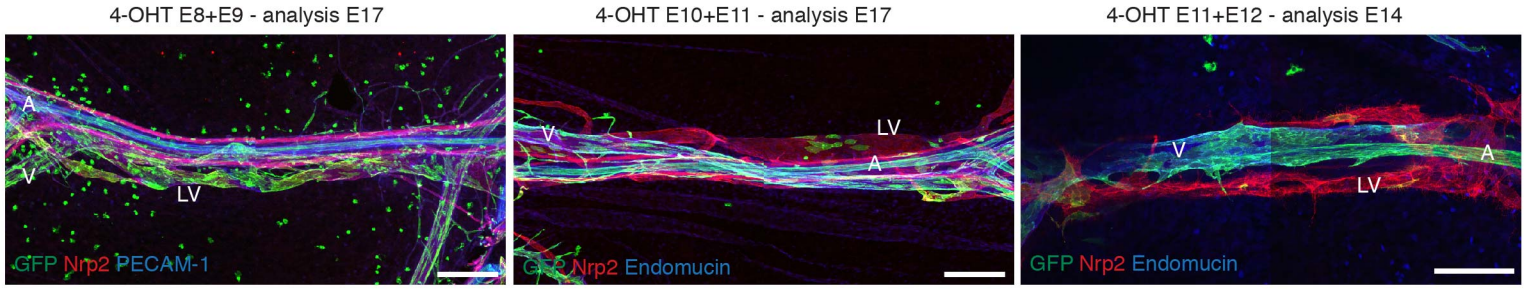

B FACS analysis of E11 *Pdgfb-CreER^{T2};R26-mTmG* whole embryo **induced at E8**

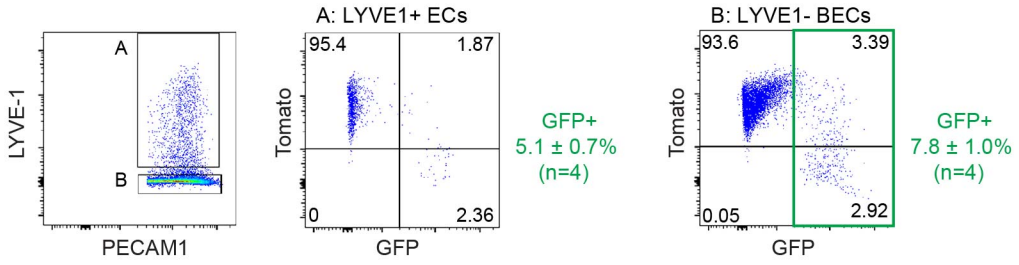

FACS analysis of E12 *Pdgfb-CreER^{T2};R26-mTmG* whole embryo **induced at E9**

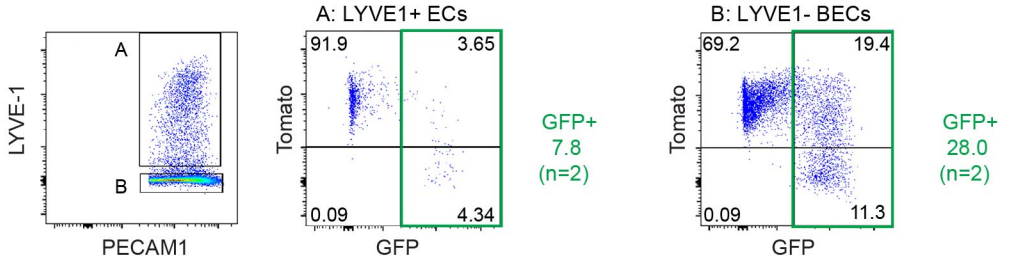

Figure S5

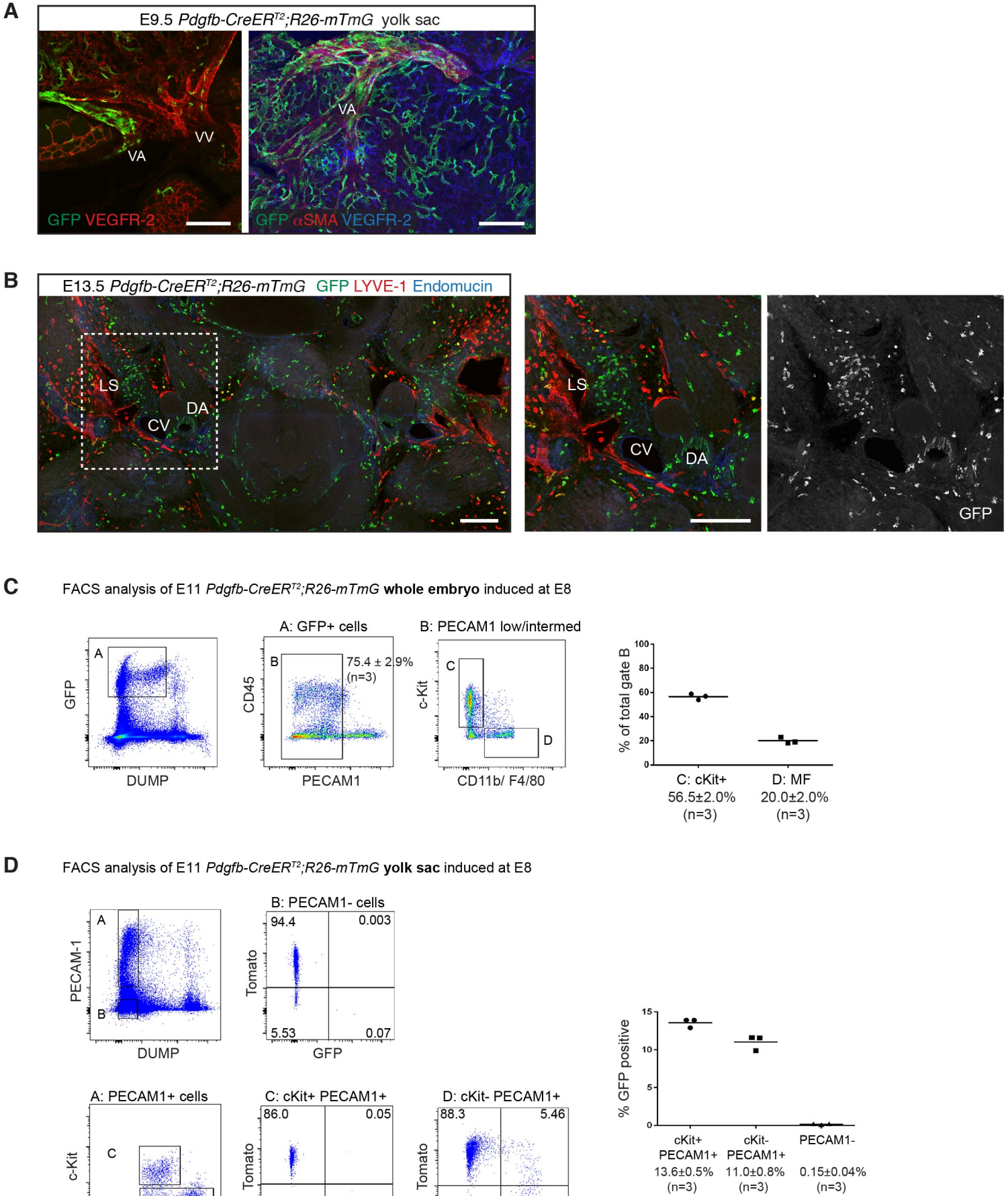
A
E9.5 Pdgfb-CreER^{T2};R26-mTmG yolk sac
VA
VV
GFP VEGFR-2
VA
GFP αSMA VEGFR-2
B
E13.5 Pdgfb-CreER^{T2};R26-mTmG GFP LYVE-1 Endomucin
LS
DA
CV
LS
CV
DA
GFP
C
FACS analysis of E11 Pdgfb-CreER^{T2};R26-mTmG whole embryo induced at E8
A: GFP+ cells
B: PECAM1 low/intermed
GFP
DUMP
CD45
PECAM1
75.4 ± 2.9%
(n=3)
c-Kit
CD11b/ F4/80
% of total gate B
C: cKit+
56.5±2.0%
(n=3)
D: MF
20.0±2.0%
(n=3)
D
FACS analysis of E11 Pdgfb-CreER^{T2};R26-mTmG yolk sac induced at E8
B: PECAM1- cells
PECAM-1
DUMP
Tomato
GFP
94.4
0.003
5.53
0.07
A: PECAM1+ cells
C: cKit+ PECAM1+
D: cKit- PECAM1+
c-Kit
PECAM1
86.0
0.05
0.11
13.8
88.3
5.46
0.13
6.14
% GFP positive
cKit+
PECAM1+
13.6±0.5%
(n=3)
cKit-
PECAM1+
11.0±0.8%
(n=3)
PECAM1-
0.15±0.04%
(n=3)

Figure S6

A

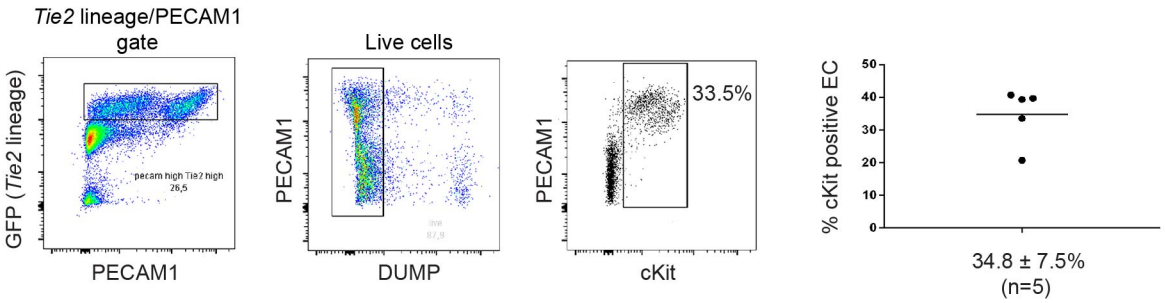
FACS analysis of E9 Tie2-Cre;R26-mTmG yolk sac
Tie2 lineage/PECAM1 gate
GFP (Tie2 lineage)
PECAM1
pecam high Tie2 high
26,5
Live cells
PECAM1
DUMP
PECAM1
33.5%
cKit
% cKit positive EC
50
40
30
20
10
0
34.8 ± 7.5%
(n=5)

B

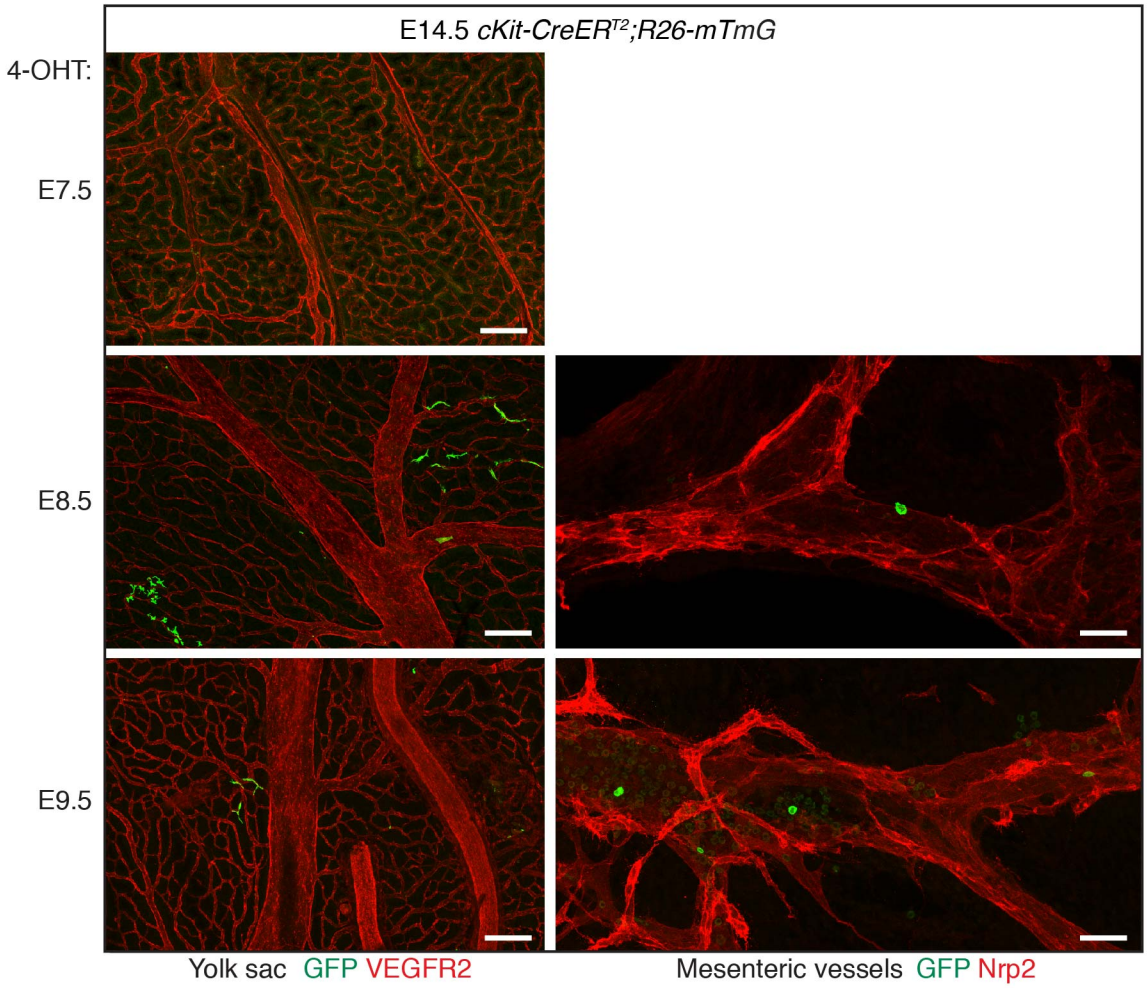
E14.5 cKit-CreER^T2;R26-mTmG
4-OHT:
E7.5
E8.5
E9.5
Yolk sac GFP VEGFR2
Mesenteric vessels GFP Nrp2

Figure S7

Supplemental Figure Legends

Figure S1, related to Figure 1. Perinatal lethality and selective inhibition of mesenteric lymphatic vessel development in *Vegfr3*$^{lz/+}$; *p110α*$^{D933A/+}$ mice.

(A) Observed and expected genotypes of embryos and mice from crosses of *p110α*$^{D933A/+}$ and *Vegfr3*$^{lz/+}$ mice. Double heterozygotes were recovered at expected Mendelian ratio before birth, but they died perinatally (highlighted in red). (B) *Vegfr3*$^{lz/+}$;*p110α*$^{D933A/+}$ pup and a wild type littermate (*Wt*) at P4. Note accumulation of chyle in the mutant intestine (arrows). (C) Mesenteries from P4 *Vegfr3*$^{lz/+}$; *p110α*$^{D933A/+}$ and littermate control mice. Lymphatic vessels were visualized by whole-mount X-Gal staining (lacZ, blue) or immunofluorescence for indicated proteins. Note diffuse leakage of chyle and rudimentary lymphatic vessels in the mesentery of mutant mice. Boxed regions show regions imaged on the right and asterisks indicate the mesenteric root. *Vegfr3*$^{lz/+}$; *p110α*$^{D933A/+}$ embryos develop only few mesenteric vessels that abnormally retain LYVE-1 expression. LV = lymphatic vessel, V = vein, A = artery, N = nerve. Scattered LYVE-1 cells are macrophages. (D) Whole-mount immunofluorescence of E17.5 intestine stained against indicated proteins. Single channel images for Prox1 are shown. (E) X-Gal stained diaphragms from P4 *Vegfr3*$^{lz/+}$; *p110α*$^{D933A/+}$ and littermate control mice showing grossly normal lymphatic network in the mutant.

Scale bars = 0.5 mm (C, left panel), 1 mm (C, middle panels; E), 100 μm (C, rightmost panel; D).

Figure S2, related to Figure 1. *Vegfr2*$^{flox/-}$;*p110α*$^{D933A/+}$ mice show no detectable phenotype in the lymphatic vasculature.

Whole-mount immunofluorescence of P4 mesenteric vasculature (A) and P21 dermal vasculature of the ear (B) stained with antibodies against indicated proteins. Arrowheads indicate lymphatic vessels.

Scale bars = 200 μm.

Figure S3, related to Figure 1. Cre-mediated recombination efficiency in the *Vegfr3-CreER*^{T2} line.

(A) FACS analysis of dermal endothelial cells from E15.5 *Vegfr3-CreER*^{T2}*;R26-mTmG* embryos showing GFP expression, indicating Cre recombination, in LECs and to a lesser extent in BECs. Representative FACS plots and gating scheme are shown and the graph of all results is shown in Figure 1E.

(B) FACS analysis of endothelial cells from E17.5 *Vegfr3-CreER*^{T2}*;R26-mTmG* mesenteries (top panels) and skin (bottom panels) showing GFP expression, indicating Cre recombination, in LECs and to a lesser extent in BECs. Representative FACS plots and gating scheme and the graph of all results are shown. The horizontal lines represent mean (n=5). For both (A) and (B) 4-OHT was administered at E10.5, E11.5, E12.5 and E13.5.

Figure S4, related to Figure 3. Characterization of mesenteric LEC clusters.

(A, B) Whole-mount immunofluorescence of E13.5 mesenteries stained with antibodies against the indicated proteins. Different stages of LEC cluster (arrows in A) and vessel formation (arrowheads in A) are observed along different artery-vein pairs within the same mesentery. Arrows in (B) indicate isolated LEC clusters negative for blood endothelial and hematopoietic markers. Arrowhead in (B) indicates CD41^{+} platelets.

Scale bars = 200 μm (A), 50 μm (B).

Figure S5, related to Figure 4. Time-course of 4-OHT induced *Pdgfb-CreER^{T2}* mediated recombination in embryonic vasculature.

(A) Time-course of 4-OHT induced Cre-mediated recombination efficiency in vascular and hematopoietic cells in *Pdgfb-CreER^{T2};R26-mTmG* mesenteries. Relative recombination efficiency in different compartments was assessed through visual scoring: +++ extensive/complete, ++ good, + poor, (+) only a few GFP^{+} cells, - no GFP^{+} cells. HC = hematopoietic cells. Note a shift in the timing of 4-OHT administration when different vessel types/HCs are most efficiently targeted; early (<E9) administration leads to efficient labeling of LECs and HCs (highlighted in red) while later (>E10) administration leads to efficient labeling of arteries and veins. Representative images of mesenteries, stained for indicated proteins, for three 4-OHT administration regimes are shown below. LV = lymphatic vessels, V = vein, A = artery.

(B) FACS analysis of endothelial cells from E11 *Pdgfb-CreER^{T2};R26-mTmG* embryos treated with 4-OHT at E8 (top panels) or E9 (bottom panels). Representative FACS plots and gating scheme are shown. Summary of results showing increased recombination efficiency in both BECs and venous-derived LECs at E9 is presented on the right side of each FACS plot. Low level of GFP expression driven by *ires-GFP* within the *Pdgfb-CreER^{T2}* transgene is detected in the BECs. Only cells expressing high levels of GFP, indicating expression from the *R26-mTmG* reporter, are included in the analysis.

Scale bars = 100 μm.

Figure S6, related to Figure 4. Characterization of Cre recombination pattern in *Pdgfb-CreER^{T2};R26-mTmG* embryos treated with 4-OHT at E8-E8.5.

(A) Whole-mount immunofluorescence of E9 *Pdgfb-CreER^{T2};R26-mTmG* yolk sac for indicated proteins. Note efficient recombination indicated by GFP expression in the vitelline artery (VA) but not the vein (VV). The identity of VA was confirmed by staining for αSMA (on the right).

(B) Whole-mount immunofluorescence of a vibratome section from E13.5 *Pdgfb-CreER^{T2};R26-mTmG* embryo for indicated proteins. Recombination, indicated by GFP expression, can be seen in the dorsal aorta (DA) and hematopoietic cells, but not in the cardinal vein (CV; Endomucin^{+}) or lymph sac (LS; LYVE-1^{+}).

(C, D) FACS analysis of endothelial cells from E11 *Pdgfb-CreER^{T2};R26-mTmG* embryo proper (C) and yolk sac (D). In the embryo, *Pdgfb-CreER^{T2}* targets mainly cKit^{+} cells and macrophages (MF) (D). In the yolk sac Cre-mediated recombination occurs in both cKit^{+}/PECAM-1^{+} hemogenic and cKit^{-}/PECAM-1^{+} non-hemogenic endothelium, but not in PECAM-1^{-} non-endothelial cells (D). Representative FACS plots and gating schemes and graphs of all results are shown. The horizontal lines represent mean.

Scale bars = 200 μm.

Figure S7, related to Figure 5. cKit expression and *cKit-CreER^{T2}* mediated Cre recombination in the yolk sac.

(A) FACS analysis of yolk sac endothelial cells from E9.5 *Tie2-Cre;R26-mTmG* embryo. cKit expression in endothelial cells (gating based on the PECAM-1^{high}GFP^{+} cell profile) is analyzed. A representative FACS plot and gating scheme and graph of all results are shown. The horizontal line represents mean (n=5).

(B) Whole-mount immunofluorescence of E14.5 *cKit-CreER^{T2};R26-mTmG* yolk sacs and mesenteries for indicated proteins, showing low recombination efficiency indicated by a small number of GFP^{+} cells. 4-OHT was administered at E7.5, E8.5 or E9.5 as indicated. Scale bars = 200 μm (yolk sacs), 50 μm (mesenteries).

Supplemental Tables

Table S1. Image acquisition details for confocal micrographs

Figure	Panel	Tile	Max intensity proj	Objective
Figure 1A	mesenteric vessel	1 x 2	yes	Plan-Apochromat 20x/0.8 NA
	lymph sac	1 x 2	yes	Plan-Apochromat 20x/0.8 NA
	skin	2 x 4	yes	C-Apochromat 10x/0.45 NA
	diaphragm		yes	Plan-Apochromat 20x/0.8 Ph2
Figure 1F	mesenteric vessel		yes	Plan-Apochromat 20x/0.8 M27
Figure 1H		3 x 5	yes	Plan-Neofluar 10x/0.30 NA
Figure 2B	E12.5		yes	Plan-Apochromat 20x/0.8 Ph2
	E13.5	1 x 2	yes	Plan-Apochromat 20x/0.8 NA
	E14.5	1 x 2	yes	Plan-Apochromat 20x/0.8 NA
Figure 2C			yes	Plan-Apochromat 20x/0.8 NA
Figure 3A		1 x 2	yes	Plan-Apochromat 20x/0.8 NA
Figure 3B			yes	Plan-Apochromat 20x/0.8
Figure 3D	VEGFR2+Prox1		yes	C-Apochromat 40x/1.20 W Korr M27
	VEGFR3+Prox1		yes	C-Apochromat 40x/1.20 W Korr M27
	Nrp2+Prox1		yes	C-Apochromat 40x/1.20 W Korr M27
	Podoplanin+Prox1		yes	Plan-Apochromat 20x/0.8
	Nrp2+Edu+Prox1		yes	C-Apochromat 40x/1.20 W Korr M27
Figure 3E			yes	Plan-Apochromat 20x/0.8
Figure 3F			yes	Plan-Apochromat 20x/0.8
Figure 3G	whole mesentery	3 x 3	yes	Plan Apochromat 10x/0.45 M27
	lymph sac		yes	Plan-Apochromat 20x/0.8
	LEC cluster		yes	Plan-Apochromat 20x/0.8
Figure 4B		1 x 2	yes	Plan-Apochromat 20x/0.8 NA
Figure 4D	whole embryo	4 x 5	yes	Plan Apochromat 10x/0.45 M27
	zoomed region		yes	Plan Apochromat 10x/0.45 M27
	section		yes	Plan Apochromat 10x/0.45 M27
Figure 5B		1 x 2	yes	Plan-Apochromat 20x/0.8 NA
Figure 5C			yes	C-Apochromat 40x/1.20 W Korr M27
Figure 6A			no	C-Apochromat 40x/1.20 W Korr M27
Figure 6C	whole mesentery	3 x 3	yes	Plan-Neofluar 10x/0.30 NA
	mesenteric vessels	1 x 2	yes	Plan-Apochromat 20x/0.8 NA
	lymph sac	2 x 2	yes	Plan Apochromat 10x/0.45 M27
	skin	2 x 4	yes	Plan-Neofluar 10x/0.30 NA
Figure S1C	mesenteric vessels		yes	Plan-Apochromat 20x/0.8
Figure S1D			yes	Plan-Apochromat 20x/0.8
Figure S2A			yes	C-Apochromat 10x/0.45 W M27
Figure S2B		3 x 2	yes	Plan-Neofluar 10x/0.30 NA
Figure S4A		7 x 6	yes	Plan-Apochromat 20x/0.8 NA
Figure S4B	Endomucin+Nrp2		yes	C-Apochromat 40x/1.20 W Korr M27
	cKit+Prox1		yes	Plan-Apochromat 20x/0.8
	ScaI+Nrp2+Prox1		yes	C-Apochromat 40x/1.20 W Korr M27
	CD41+Nrp2+Prox1		yes	C-Apochromat 40x/1.20 W Korr M27
	CD45+Nrp2+Prox1		yes	C-Apochromat 40x/1.20 W Korr M27
Figure S5A	4OHT E8+E9	1 x 2	yes	Plan-Neofluar 10x/0.30
	4OHT E10+E11	1 x 2	yes	Plan-Neofluar 10x/0.30
	4OHT E11+E12	1 x 2	yes	Plan-Apochromat 20x/0.8 Ph2
Figure S6A	left		yes	Plan Apochromat 10x/0.45 M27
	right	2 x 2	yes	Plan Apochromat 10x/0.45 M27
Figure S6B		2 x 4	yes	Plan Apochromat 10x/0.45 M27
Figure S7B	yolk sacs	3 x 2	yes	Plan-Apochromat 10x/0.45 M27
	mesenteric vessels	1 x 2	yes	Plan-Apochromat 20x/0.8 NA

Supplemental Experimental Procedures

Mice

R26-mTmG (Muzumdar et al., 2007) mice were obtained from the Jackson Laboratory. *Vegfr3-CreER^{T2}* (I.M-C. and S.O., unpublished) will be published elsewhere. Transgenic mouse expressing EGFP under the control of the Claudin5 promoter/enhancer (*Cldn5-GFP*) was generated by B.L. and C.B. (unpublished). *Tie2-Cre* (Koni et al., 2001), *Pdgfb-CreER^{T2}* (Claxton et al., 2008), *cKit-CreER^{T2}* (Klein et al., 2013), *Pdgfrb-Cre* (Foo et al., 2006), *Vav-Cre* (de Boer et al., 2003), *Vegfr3^{flox}* (Haiko et al., 2008), *Vegfr3^{lz}* (Dumont et al., 1998), *p110α^{flox}* (Graupera et al., 2008) and *p110α^{D933A}* (Foukas et al., 2006) lines have been described previously. *Vegfr3$^{lz/+}$;p110α$^{D933A/+}$* embryos and pups were generated from crosses of heterozygous parents. *Vegfr2$^{+/-}$* mice were generated by crossing *Vegfr2^{flox}* (Haigh et al., 2003) with the *PGK-Cre* mice, followed by crossing with C57BL/6J mice to remove the Cre transgene. *Vegfr2$^{flox/-}$;p110α$^{D933A/+}$* embryos and pups were generated from crosses of *Vegfr2$^{+/-}$;p110α$^{D933A/+}$* and *Vegfr2$^{flox/flox}$* mice.

Antibodies

The following antibodies were used for immunofluorescence: rabbit anti-GFP (Invitrogen), hamster anti-mouse Podoplanin (Developmental Studies Hybridoma Bank), rabbit anti-human Prox1 (generated against human Prox1 C-terminus (567-737aa), Prox1-GST construct provided by Dr. T. Petrova, University of Lausanne), rat anti-mouse Endomucin (Santa Cruz Biotechnology), chicken anti-GFP, rat anti-mouse CD45, rat anti-mouse SCA1 (all from Abcam), rat anti-mouse PECAM-1, rat anti-mouse CD41, rat anti-mouse CD34 (all from

BectonDickinson), rat anti-mouse LYVE-1, goat anti-mouse c-KIT, goat anti-mouse Nrp2, goat anti-mouse VEGFR-2, goat anti-mouse VEGFR-3 (all from R&D Systems). Secondary antibodies conjugated to DyLight 405, Cy2, Cy3 or Cy5 were obtained from Jackson ImmunoResearch.

For FACS analysis, skin samples were stained with anti-LYVE-1 (ALY7) eF660 and anti-CD31/PECAM-1 (390) PE-Cy7, (both eBioscience). For E13 mesenteries, rat-anti podoplanin eF660 (eBio8.1.1) (eBioscience) was also added, to allow detection of non-LYVE1 positive LECs. Dump channel included anti-CD45 (30-F11) e450, anti-F4/80 (BM8) e450, anti-TER-119 (TER-119) eF450, anti-CD11b (M1/70) eF450 (all eBioscience) to exclude non-stromal cells and Sytox blue (Life technologies) to exclude non-viable cells. Yolk sacs and embryos were stained with different combinations of anti-CD31/PECAM-1 (390) PE-Cy7, anti-LYVE-1 (ALY7) eF660, anti-CD117 (2B8) APC or PERCP-eF710, anti-CD45 (30-F11) PERCP-Cy5.5. The dump channel included anti-F4/80 (BM8) eF450, anti-CD11b (M1/70) eF450, anti-TER-119 (TER-119) eF450 (all eBioscience) to exclude macrophages and red blood cells, together with Sytox blue (Life technologies) to exclude non-viable cells.

Quantification

Mesenteric lymphatic vessel phenotype was quantified by counting the proportion of artery-vein pairs (n=3-6 per embryo) extending from the mesenteric root to the intestine that were accompanied by lymphatic vessel(s) and presented as lymphatic vessel coverage: absent (no lymphatic vessels), <50% (less than half), ≥50% (more than half) and 100% (all artery-vein pairs accompanied by lymphatic vessel). Only continuous vascular structures connected to

the mesenteric root were considered as vessels. Control mice and embryos showed 100% coverage. The presence and size of the mesenteric lymph sac (absent, reduced size, normal size) was determined by comparison to littermate controls. Unless specified otherwise, controls represent littermate mice and embryos from different genotypes (single heterozygous, Cre-negative or wild type) that did not show a phenotype and were grouped.

Quantification of lymphatic vessel sprouting was done using LSM Image Browser (Zeiss) from maximum intensity projection images of tile scanned E17.5 skins (xy = 3400 µm x 1700 µm, upper thoracic region). The length of the sprout was calculated in relation to the dorsal midline. Dorsal midline was marked with a line. A distance of 1352 µm was measured laterally from the midline and the sprouting distance was calculated from the laterally located line to vessel tip. From each image 6-8 measurements were taken, 3-4 on each side of the midline. Quantification of lymphatic vessel branching was done from maximum intensity projection images of tile scanned E15.5 skins (xy = 3400 µm x 1700 µm, upper thoracic region) stained for Nrp2. All branch points per each image were marked using Photoshop CS5.1 software and counted manually.

For quantification of nuclear morphology the length/width ratio was measured for each $Prox1^+$ nuclei using ImageJ software. A total of 135 $Prox1^+$ cells were analyzed from lymphatic clusters (n=5 embryos), 123 from lymph sacs (n=2 embryos) and 141 from lymphatic vessels (n=5 embryos). For *Pdgfrb-Cre* lineage tracing, the number of GFP^+Prox1^+ cells versus all $Prox1^+$ cells within isolated LEC clusters was counted manually (n=24 clusters containing 2-12 cells each, from 3 embryos).

Quantification of GFP fluorescence intensity in endothelial cells of *Cldn5-GFP* mesenteries

was done using ImageJ software. Three measurements per cell were taken using the point tool and mean value was calculated. Background intensity value was similarly measured in each image and subtracted from the cell measurements. Total number of $Prox1^{+}$ cells measured was 27 (single cells), 23 (clusters of 2 cells), 38 (clusters of 3-4 cells) from 3 embryos.

In vivo cell proliferation assay

Click-iT Edu Imaging Kit (Invitrogen) was used to detect proliferating cells. Pregnant females were administered with 0.7 mg of Edu in PBS by intraperitoneal injection 5 hours prior to embryo dissection. Embryonic mesenteries were dissected, fixed, permeabilized and blocked with 3% milk in PBSTx as described above. Tissue was washed in PBS for 10 minutes at RT and incubated in the Click-iT reaction cocktail for 1 hour at room temperature followed by washes in PBS and staining with primary and secondary antibodies as described previously.

Detection of β-galactosidase activity by X-gal staining

The mesentery and diaphragm from *Vegfr3*$^{lz/+}$ mice were dissected and rinsed in 0.1M sodium phosphate buffer (pH 7.3) followed by incubation in the fixative (94mM sodium phosphate buffer pH 7.3 with 0.2% glutaraldehyde, 5mM EGTA pH 7.3, 2mM MgCl2,) for 30 minutes at RT. The tissues were washed three times in the wash buffer (0.1M sodium phosphate buffer pH 7.3 with 2mM MgCl2, 0.01% w/v deoxycholic acid, 0.02% NP-40) for 15 minutes each time at RT. Tissues were stained in X-gal staining solution (0.1% w/v X-gal, 0.212% w/v potassium ferrocyanide, 0.164% w/v potassium ferricyanide, in wash buffer)

overnight at 37°C. The following day, stained tissues were washed three times in the wash buffer for 15 minutes each time at RT then post-fixed in 4% PFA for approximately 8 hours at 4°C and stored in PBS at 4°C.

References

Claxton, S., Kostourou, V., Jadeja, S., Chambon, P., Hodivala-Dilke, K., and Fruttiger, M. (2008). Efficient, inducible Cre-recombinase activation in vascular endothelium. Genesis *46*, 74-80.

de Boer, J., Williams, A., Skavdis, G., Harker, N., Coles, M., Tolaini, M., Norton, T., Williams, K., Roderick, K., Potocnik, A.J.*, et al.* (2003). Transgenic mice with hematopoietic and lymphoid specific expression of Cre. Eur J Immun *33*, 314-325.

Dumont, D.J., Jussila, L., Taipale, J., Lymboussaki, A., Mustonen, T., Pajusola, K., Breitman, M., and Alitalo, K. (1998). Cardiovascular failure in mouse embryos deficient in VEGF receptor-3. Science *282*, 946-949.

Foo, S.S., Turner, C.J., Adams, S., Compagni, A., Aubyn, D., Kogata, N., Lindblom, P., Shani, M., Zicha, D., and Adams, R.H. (2006). Ephrin-B2 controls cell motility and adhesion during blood-vessel-wall assembly. Cell *124*, 161-173.

Foukas, L.C., Claret, M., Pearce, W., Okkenhaug, K., Meek, S., Peskett, E., Sancho, S., Smith, A.J., Withers, D.J., and Vanhaesebroeck, B. (2006). Critical role for the p110alpha phosphoinositide-3-OH kinase in growth and metabolic regulation. Nature *441*, 366-370.

Graupera, M., Guillermet-Guibert, J., Foukas, L.C., Phng, L.K., Cain, R.J., Salpekar, A., Pearce, W., Meek, S., Millan, J., Cutillas, P.R.*, et al.* (2008). Angiogenesis selectively

requires the p110alpha isoform of PI3K to control endothelial cell migration. Nature *453*, 662-666.

Haigh, J.J., Morelli, P.I., Gerhardt, H., Haigh, K., Tsien, J., Damert, A., Miquerol, L., Muhlner, U., Klein, R., Ferrara, N.*, et al.* (2003). Cortical and retinal defects caused by dosage-dependent reductions in VEGF-A paracrine signaling. Dev Biol *262*, 225-241.

Haiko, P., Makinen, T., Keskitalo, S., Taipale, J., Karkkainen, M.J., Baldwin, M.E., Stacker, S.A., Achen, M.G., and Alitalo, K. (2008). Deletion of vascular endothelial growth factor C (VEGF-C) and VEGF-D is not equivalent to VEGF receptor 3 deletion in mouse embryos. Mol Cell Biol *28*, 4843-4850.

Klein, S., Seidler, B., Kettenberger, A., Sibaev, A., Rohn, M., Feil, R., Allescher, H.D., Vanderwinden, J.M., Hofmann, F., Schemann, M.*, et al.* (2013). Interstitial cells of Cajal integrate excitatory and inhibitory neurotransmission with intestinal slow-wave activity. Nat Commun *4*, 1630.

Koni, P.A., Joshi, S.K., Temann, U.A., Olson, D., Burkly, L., and Flavell, R.A. (2001). Conditional vascular cell adhesion molecule 1 deletion in mice: impaired lymphocyte migration to bone marrow. J Exp Med *193*, 741-754.

Muzumdar, M.D., Tasic, B., Miyamichi, K., Li, L., and Luo, L. (2007). A global double-fluorescent Cre reporter mouse. Genesis *45*, 593-605.